nature Vol 460|16 July 2009|doi:10.1038/nature08163

LETTERS

Evidence for middle Eocene Arctic sea ice from diatoms and ice-rafted debris

Catherine E. Stickley[1,3], Kristen St John[2], Nalân Koç[1,3], Richard W. Jordan[4], Sandra Passchier[5], Richard B. Pearce[6] & Lance E. Kearns[2]

Oceanic sediments from long cores drilled on the Lomonosov ridge, in the central Arctic[1], contain ice-rafted debris (IRD) back to the middle Eocene epoch, prompting recent suggestions that ice appeared in the Arctic about 46 million years (Myr) ago[2,3]. However, because IRD can be transported by icebergs (derived from land-based ice) and also by sea ice[4], IRD records[2,3] are restricted to providing a history of general ice-rafting only. It is critical to differentiate sea ice from glacial (land-based) ice as climate feedback mechanisms vary and global impacts differ between these systems: sea ice directly affects ocean–atmosphere exchanges[5], whereas land-based ice affects sea level and consequently ocean acidity[6]. An earlier report[3] assumed that sea ice was prevalent in the middle Eocene Arctic on the basis of IRD, and although somewhat preliminary supportive evidence exists[2], these data are neither comprehensive nor quantified. Here we show the presence of middle Eocene Arctic sea ice from an extraordinary abundance of a group of sea-ice-dependent fossil diatoms (*Synedropsis* spp.). Analysis of quartz grain textural characteristics further supports sea ice as the dominant transporter of IRD at this time. Together with new information on cosmopolitan diatoms and existing IRD records[2], our data strongly suggest a two-phase establishment of sea ice: initial episodic formation in marginal shelf areas ~47.5 Myr ago, followed ~0.5 Myr later by the onset of seasonally paced sea-ice formation in offshore areas of the central Arctic. Our data establish a 2-Myr record of sea ice, documenting the transition from a warm, ice-free[3] environment to one dominated by winter sea ice at the start of the middle Eocene climatic cooling phase[7].

Current thinking suggests that the Cenozoic cryosphere evolved in phases, starting in the late–middle Eocene with the presence of small, isolated ice caps in both hemispheres[8–10], and interrupted by at least one short warming event[11] before major ice-sheet expansion on Antarctica and concomitant deep-sea cooling in the late Eocene and early Oligocene[7–9]. Much of the focus has been on land-based ice, but sea ice is an integral part of past and present cryospheric systems as it is involved in important climate feedbacks, such as changes in the global energy budget through the albedo effect[5,8]. Yet relatively little is known of the temporal and geographic distribution of sea ice before the Quaternary, largely because its effects are expressed more subtly and, arguably, less widely in the geological record than those of land-based ice. Part of the problem is that transient or localized sea ice may leave no obvious sedimentary record, or that its effects are easily overlooked. Application of one of the conventional methods for tracing past sea ice, using sea-ice-associated diatoms in marine sediments[12], is less obvious for the pre-Quaternary and is certainly challenging for the current patchy Eocene diatom record, particularly in Antarctica (Supplementary Information).

In the Arctic, pre-Quaternary sea-ice patterns are beginning to be understood through the Integrated Ocean Drilling Program Expedition 302 ('ACEX'), which recovered the first long Cenozoic palaeoceanographic record from the Lomonosov ridge in the central Arctic[1,3,13] (Fig. 1). It is now known, for example, that episodic perennial sea ice first appeared in the middle Miocene[14,15]. Here we present evidence for middle Eocene seasonal sea ice from a ~2-Myr-long record of fossil sea-ice diatoms and sea-ice-dominated IRD; this record is contained within a ~36-m interval of finely laminated, organic-rich, biosiliceous sediments[1,16] that represent the start of Cenozoic cooling following the Early Eocene Climatic Optimum[7] (Supplementary Fig. 1). These sediments contain abundant marine and freshwater siliceous and organic-walled microfossils[1,16–18], including diverse and largely endemic diatom assemblages characterized by heavily silicified marine Palaeogene taxa such as *Hemiaulus* spp.[1,16] and *Anaulus arcticus*[18].

Figure 1 | Idealized palaeogeography of the Arctic region for the early middle Eocene during the phase of biosilica production and preservation at the Lomonosov ridge (~50–45 Myr ago). Redrawn from ref. 17 with the difference that the Turgay Strait (outlined) is essentially closed to any major exchange at this time, based on siliceous microfossil data (Supplementary Information).

[1]Department of Geology, University of Tromsø, N-9037 Tromsø, Norway. [2]Department of Geology and Environmental Science, James Madison University, Harrisonburg, Virginia 22807, USA. [3]Norwegian Polar Institute, Polar Environmental Centre, N-9296 Tromsø, Norway. [4]Department of Earth and Environmental Sciences, Yamagata University, Yamagata 990-8560, Japan. [5]Department of Earth and Environmental Studies, Montclair State University, Montclair, New Jersey 07043, USA. [6]National Oceanography Centre, Southampton, University of Southampton, Southampton SO14 3ZH, UK.

Above 260.30 m composite depth (m.c.d.), weakly silicified, araphid, needle-shaped pennate diatoms *Synedropsis* spp. (Figs 2 and 3; Supplementary Figs 2–4) are preserved in abundances typically exceeding 25%, but reaching as high as ~61% of the diatom assemblage. Previously overlooked in initial investigations[1], these are some of the most delicately silicified diatoms discovered in the fossil record, with preservation so remarkable that micro-aggregate and colony integrity is commonly still intact (Supplementary Information). Sediment trap studies show that most diatom valves do not reach the sea floor because normal sea water is under-saturated in silica, making opaline (amorphous hydrous) silica—that impregnates the diatom cell-wall—highly susceptible to dissolution and biasing diatom records towards relatively large or heavily silicified types[19]. Weakly silicified diatoms are preserved only under exceptional circumstances, and are particularly unusual for Palaeogene sediments. In this respect, the ACEX diatom record is unprecedented and reflects a most unusual environmental setting. We attribute the preservation of *Synedropsis* spp. in these sediments to the presence of sea ice and silica-enriched waters.

Today, colonies of extant *Synedropsis* spp. are peculiar to polar sea ice[20] (Supplementary Information). The ACEX fossil *Synedropsis* spp. are uniquely associated with the middle Eocene IRD record from the same cores (Fig. 3), and here we demonstrate that this IRD record is predominantly derived from sea ice. On the basis of this association and by analogy with living *Synedropsis* spp., including the manner in which they are preserved (Supplementary Information), we propose that the ACEX *Synedropsis* spp. were, like their modern counterparts, sea-ice-dependent and, as such, highly specialized extremophiles, uniquely adapted for surviving the lengthy polar darkness and freezing temperatures. These diatoms provide the most compelling evidence for ancient sea ice, as they rely on this medium for their survival. Furthermore, the ACEX *Synedropsis* spp. represent the earliest known fossil record of sea-ice diatoms (Supplementary Information). Also we found no reports in the literature of *Synedropsis* spp. (or of any synonyms[20] or misidentifications) in pre-Holocene sediments from elsewhere in the Arctic and subarctic regions, suggesting their geographic and stratigraphic limitation.

The presence of *Synedropsis* spp. in the ACEX sediments shows that non-permanent (for example, seasonal) sea ice existed over the

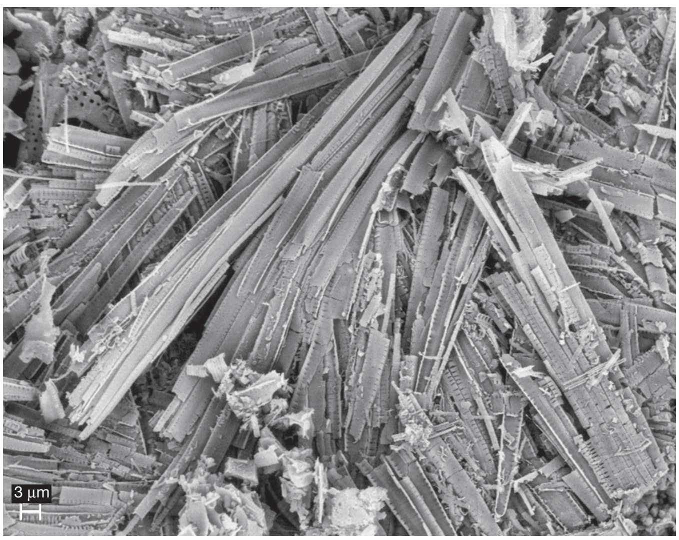

Figure 2 | SEM image of part of an aggregate of near-whole needle-shaped *Synedropsis* sp. valves. Imaged along a lamina-parallel fracture (topographic) surface of unprocessed core material at 240.90 m.c.d. (302-2A-55X5, 19.5 cm; 46.16 Myr ago). The main part of the image shows most valves are missing just the apices. Valves that have been fractured in several places are visible in the lower left and upper right corners of this image. Scale bar, 3 µm. Images of colonies, aggregates, and details of the apices are shown in Supplementary Figs 3 and 4.

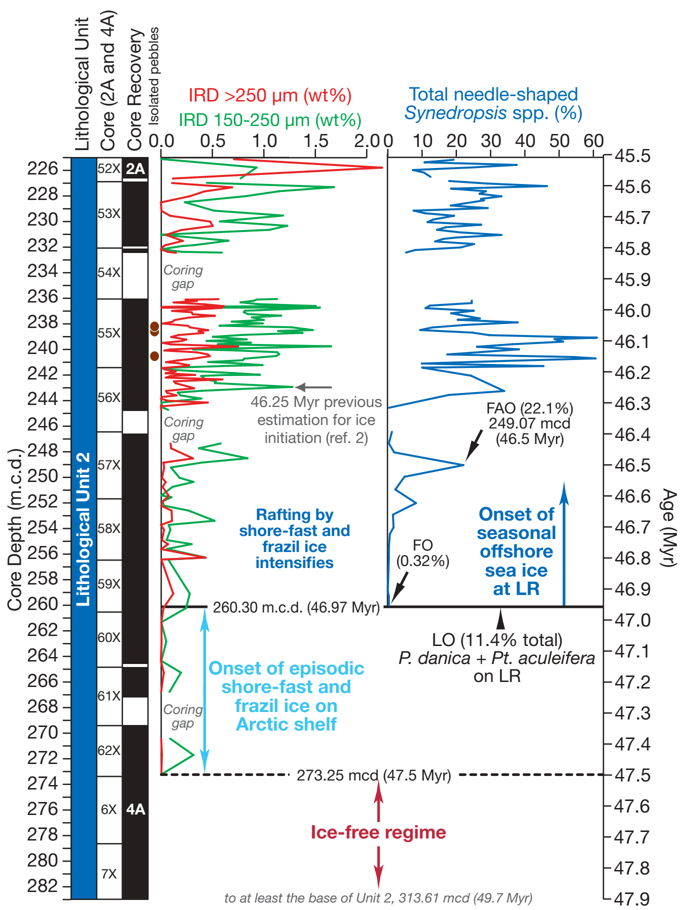

Figure 3 | IRD and sea-ice diatom abundance in the ACEX cores. Shown are data for the >250 µm (red) and 150–250 µm (green) quartz fractions, and the relative abundance (percentage of total diatoms) of needle-shaped *Synedropsis* spp. (blue). Over the age range shown, shallow exchange between the Lomonosov ridge and the proto-Norwegian-Greenland sea remains possible year-round until 46.97 Myr ago, but becomes seasonally restricted at younger ages. FO, first occurrence; FAO, first abundant occurrence; LO, last occurrence; LR, Lomonosov ridge. IRD data are from ref. 2. Age model is from ref. 13.

Lomonosov ridge, and that regular (for example, annual) melting episodes, into silica-enriched waters, permitted their preservation. It is likely that sea ice formed in autumn and winter and melted in spring and summer, as seasonal sea ice does today. We suggest that *Synedropsis* spp. over-wintered within the sea ice and later bloomed there after irradiance increased in the following spring. Following sea-ice melt, they were released into stratified surface waters where aggregation was undoubtedly intensified by virtue of their stickiness[21] and needle shape. As aggregation enhances sinking rates, these were unlikely candidates for seeding the melt zone[21]. We therefore suggest they did not constitute a significant part of the summer growth alongside other diatom taxa. Instead, they underwent rapid flux to the sea floor where they remained largely undisturbed under an anoxic benthic environment[16,22]. Such sea-ice-driven seasonality is evident from our preliminary investigations of the laminations that indicate *Synedropsis* spp. form regularly occurring, near-monogeneric laminations, commonly associated with IRD. This indicates that production and flux of sea-ice diatoms occurred at a different stage in the annual cycle to that of the other ACEX diatoms, and that *Synedropsis* spp. laminations probably represent episodes of spring or summer sea-ice melt and flux, a hypothesis necessitating examination of the lamination sequences through the core.

The current estimate for the initiation of ice in the Arctic is ~46.25 Myr ago[2] (Fig. 3), based on IRD evidence only, in particular on the doubling of sand-sized IRD flux to 0.02 g cm^{-2} kyr^{-1} and establishment of a quasi-cyclicity[2]. However, IRD exists in the ACEX cores as far back as ~47.5 Myr ago[2] (Fig. 3), albeit in low abundance. *Synedropsis* spp. appear in the record 46.97 Myr ago, thereafter co-varying with IRD throughout the biosilica-rich core sections (Supplementary Fig. 2). The appearance of *Synedropsis* spp. in the ACEX cores coincides with the disappearance of a cosmopolitan (warmer water) diatom component characterized by *Porotheca danica* and *Pterotheca aculeifera* (Fig. 3), whereas other endemic taxa persist throughout the cores. Considering that the IRD record is largely derived from sea-ice transportation (as we show here), the timing of this floral turnover strongly suggests a two-phase establishment of middle Eocene Arctic sea ice (Fig. 3).

We propose that the onset of IRD in the ACEX cores ~47.5 Myr ago marks the onset of shore-fast ice and/or frazil ice, forming up-current in one or more shallow areas of the broad marginal Arctic shelf, which entrained and (via wind-driven surface currents) transported sand-sized terrigenous material to the central Arctic. Marginal sea-ice formation was likely to have been episodic, based on the low abundance of IRD (Fig. 3) and the absence of sea-ice diatoms in this phase (Supplementary Information). We further propose that the appearance of well-preserved, lamina-forming sea-ice diatoms and the concurrent disappearance of cosmopolitan diatoms ~47 Myr ago marks the onset of seasonally paced offshore sea-ice formation—for example, pack ice. It is conceivable that—under generally declining middle Eocene temperatures and atmospheric carbon dioxide (CO_2) levels (refs 23, 24)—sea ice would have formed initially at the margins, later advancing into offshore areas of the Arctic Ocean, to include at least the surface-waters above, or close to, the palaeo-location of the ACEX drillsite (Fig. 1). A parallel increase in IRD (Fig. 3) indicates that ice-rafting of shallow shelf sediments intensified at the same time.

Before ~47 Myr ago, year-round shallow oceanic exchange between the Lomonosov ridge and the proto-Norwegian-Greenland Sea was possible, indicated by the presence of *P. danica* and *Pt. aculeifera* in coeval sediments from this area. Once an offshore seasonal sea-ice regime was established, the northern limit of ice-intolerant cosmopolitan diatoms was driven southwards, and the potential for shallow oceanic exchange became restricted to the summer melt season.

Our data provide compelling evidence for the establishment of an offshore winter sea-ice regime ~47 Myr ago that was stable enough to support an ecology and persistent enough to cause the southward migration of cosmopolitan taxa. Sea-ice-driven positive climate feedbacks, such as reduced oceanic heat loss to the atmosphere and enhanced albedo—by sea ice[5] (in spring) and cloud formation[25] (in summer)—would therefore have become particularly important at this time. A stable sea-ice regime also suggests the possibility of concomitant glacial ice. If glaciers were also present, then an understanding of the relative contribution of both sea ice-IRD and iceberg-IRD is essential.

A possible discriminator in the Arctic is quantitative analysis of the surface textures of ice-rafted quartz grains[26], using a statistical approach[27]. IRD grains exhibiting both sea-ice and iceberg textures are present in a short study interval (~236–242 m.c.d.; Fig. 4). Discriminant scores are significantly different for the two groups with 93% correctly classified, although some overlap exists between the populations (Supplementary Fig. 5). Our data indicate that sea ice was the dominant mode of ice transport between ~46.2 Myr and ~46.0 Myr ago. Before ~46.15 Myr ago (240.53 m.c.d.), 80–100% of the grains exhibit sea-ice textures (0–20% iceberg-IRD textures). The highest input of iceberg-IRD occurs ~46.15 Myr ago, after which peaks in iceberg-IRD broadly correspond to peaks in total IRD abundance (Fig. 4). This suggests the presence of small isolated glaciers that pre-date estimates for those on Greenland (~38 Myr or ~44 Myr ago, refs 10 and 28 respectively), in keeping with results of a global climate/ice-sheet model[9]; this model shows the potential for small isolated ice caps on higher Arctic elevations in the Eocene

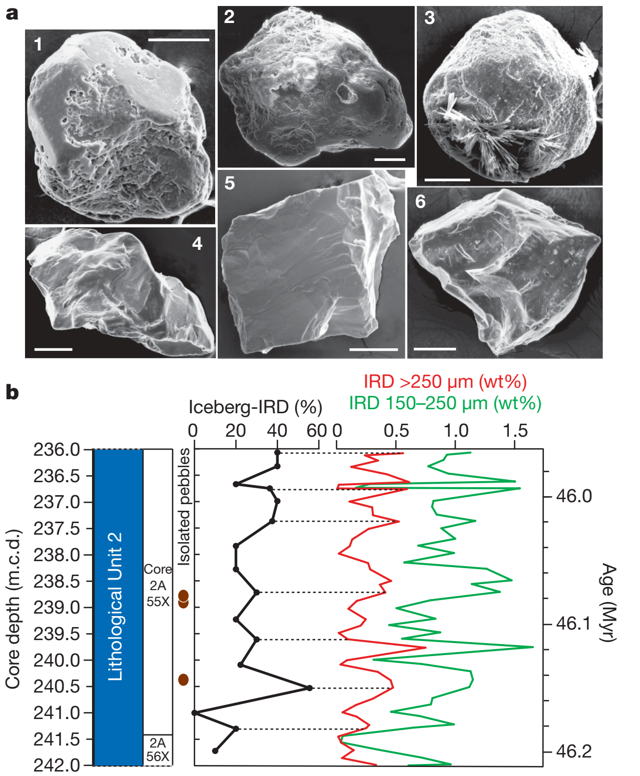

Figure 4 | Results of IRD analysis in a short core interval. a, SEM images of IRD with textural characteristics of sea-ice transport (upper row) and iceberg transport (lower row). **b,** Percentage of iceberg-rafted versus sea-ice-rafted quartz sand (>250 μm) and correlation with IRD abundance. Details are provided in Supplementary Information.

and Oligocene, and no major glaciation until ~23 Myr ago or later[9]. Nevertheless, even where total IRD input is high, 60–80% of grains are classified as sea ice-IRD, confirming the importance of sea ice in the middle Eocene Arctic.

The ACEX middle Eocene sea-ice record pre-dates known major Cenozoic glacial and sea-ice records, which has two intriguing consequences: (1) the current 'icehouse' cryosphere started to evolve earlier than previously thought; and (2) significant sea ice formed in the central Arctic some ~24 Myr before major ice-sheet expansion in the region[9]. Therefore, sea ice–ice sheet linkages, such as those surmised for Cenozoic Antarctica[5], could not have existed in the middle Eocene Arctic. Furthermore, together with results of a numerical model for Cenozoic Antarctic climate evolution[5], and known Cenozoic Antarctic sea-ice records (Supplementary Information), our data indicate that sea ice formed in the Arctic before it did in Antarctica. Under generally declining middle Eocene atmospheric CO_2 (refs 23, 24), this implies that the threshold for sea-ice formation was crossed in the Arctic first, a hypothesis opposite to that modelled for glacial ice, whereby Antarctica is shown to glaciate much earlier (that is, at higher levels of CO_2) than circum-Arctic continents[9].

Arctic palaeogeography and palaeoenvironments may ultimately account for these consequences. Strong salinity stratification[16,22] prevailed within a basin essentially isolated from the world's oceans (Fig. 1), where low surface salinities[29,30] appreciably facilitated annual freezing. A notable influx of fresh water[30] and subsequent fall in salinity starting ~47.6 Myr (refs 29, 30) or ~47.2 Myr (ref. 16) ago strongly suggests salinity-controlled preconditioning just before and during sea-ice initiation.

METHODS SUMMARY

Quantitative diatom analysis. Dried sediment samples from the interval ~201–302 m.c.d. (cores 302 2A 47X to 4A 11X) were weighed to a value between

~0.1–0.2 g, processed for biogenic silica and analysed using the quantitative and light microscopy methodologies outlined elsewhere[16]. Sampling resolution was at an average of ~20 cm over critical intervals (otherwise at every ~30–100 cm excluding coring gaps). Light microscope images were taken using a Panasonic DMC-FS5 camera at ISO 1600 and at ×1,000 magnification. Further aliquots were dried onto aluminium scanning electron microscope (SEM) stubs, gold sputter coated and imaged using an LEO 1450VP SEM at 15–20 kV. Lamina-parallel fracture (topographic) surfaces of unprocessed core material were also imaged in the SEM.

Quantitative IRD abundance. We followed previously outlined methods[2].

Quantitative IRD surface texture analysis. We analysed 160 grains; 10 quartz grains from the >250 µm size range were randomly picked for SEM imaging from each of 16 samples between ~236 and 242 m.c.d. (cores 302 2A 55X-56X). This interval was selected for its good core recovery[1], good age control[13], robust IRD record[2], and for encompassing the oldest recorded dropstone[1–3] ('isolated pebbles' on Figs 3 and 4 and Supplementary Fig. 2). Samples were analysed using an LEO 1430VP SEM. Elemental (EDS) analysis verified that each grain was quartz. Statistical analysis included principal component analysis (PCA) and discriminant analysis[27].

Full Methods and any associated references are available in the online version of the paper at www.nature.com/nature.

Received 5 January; accepted 21 May 2009.

1. Backman, J., Moran, K., McInroy, D. B., Mayer, L. A. & the Expedition 302 Scientists. *Proc. IODP* **302,** doi:10.2204/iodp.proc.302.2006 (2006).
2. St John, K. Cenozoic ice-rafting history of the central Arctic Ocean: terrigenous sands on the Lomonosov Ridge. *Paleoceanography* **23,** PA1S05, doi:10.1029/2007PA001483 (2008).
3. Moran, K. *et al.* The Cenozoic palaeoenvironment of the Arctic Ocean. *Nature* **441,** 601–605 (2006).
4. Nurnberg, D. *et al.* Sediments in Arctic sea ice: implications for entrainment, transport, and release. *Mar. Geol.* **119,** 185–214 (1994).
5. DeConto, R., Pollard, D. & Harwood, D. Sea ice feedback and Cenozoic evolution of Antarctic climate and ice sheets. *Paleoceanography* **22,** PA3214, doi:10.1029/2006PA001350 (2007).
6. Merico, A., Tyrrell, T. & Wilson, P. A. Eocene/Oligocene ocean de-acidification linked to Antarctic glaciation by sea level fall. *Nature* **452,** 979–982 (2008).
7. Zachos, J. *et al.* Trends, rhythms, and aberrations in global climate 65 Ma to present. *Science* **292,** 686–693 (2001).
8. DeConto, R. M. & Pollard, D. Rapid Cenozoic glaciation of Antarctica induced by declining atmospheric CO_2. *Nature* **421,** 245–249 (2003).
9. DeConto, R. M. *et al.* Thresholds for Cenozoic bipolar glaciation. *Nature* **455,** 652–656 (2008).
10. Eldrett, J. S. *et al.* Continental ice in Greenland during the Eocene and Oligocene. *Nature* **466,** 176–179 (2007).
11. Bohaty, S. M. *et al.* Coupled greenhouse warming and deep-sea acidification in the middle Eocene. *Paleoceanography* **24,** PA2207, doi:10.1029/2008PA001676 (2009).
12. Armand, L. K. & Leventer, A. in *Sea Ice: An Introduction to its Physics, Chemistry, Biology and Geology* (eds Thomas, D. N. & Dieckmann, G. S.) 333–372 (Blackwell Science, 2003).
13. Backman, J. *et al.* Age model and core-seismic interpretation for the Cenozoic Arctic Coring Expedition sediments from the Lomonosov Ridge. *Paleoceanography* **23,** PA1S03, doi:10.1029/2007PA001476 (2008).
14. Darby, D. A. Arctic perennial ice cover over the last 14 million years. *Paleoceanography* **23,** PA1S07, doi:10.1029/2007PA001479 (2008).
15. Krylov, A. A. *et al.* A shift in heavy and clay mineral provenance indicates a middle Miocene onset of a perennial sea ice cover in the Arctic Ocean. *Paleoceanography* **23,** PA1S06, doi:10.1029/2007PA001497 (2008).
16. Stickley, C. E. *et al.* A siliceous microfossil view of middle Eocene Arctic environments: a window of biosilica production and preservation. *Paleoceanography* **23,** PA1S14, doi:10.1029/2007PA001485 (2008).
17. Brinkhuis, H. *et al.* Episodic fresh surface waters in the early Eocene Arctic Ocean. *Nature* **441,** 606–609 (2006).
18. Suto, I., Jordan, R. W. & Watanabe, M. Taxonomy of middle Eocene diatom resting spores and their allied taxa from IODP sites in the central Arctic Ocean (the Lomonosov Ridge). *Micropaleontology* **55,** 259–312 (2009).
19. Barron, J. A. & Baldauf, J. G. in *Siliceous Microfossils* (eds Blome, C. D. *et al.*) 107–118 (Short Courses in Paleontology, Vol. 8, Paleontological Society, 1995).
20. Hasle, G. R., Medlin, L. K. & Syvertsen, E. E. *Synedropsis* gen. nov., a genus of araphid diatoms associated with sea ice. *Phycologia* **33,** 248–270 (1994).
21. Riebesell, U., Schloss, I. & Smetacek, V. Aggregation of algae released from melting sea ice: implications for seeding and sedimentation. *Polar Biol.* **11,** 239–248 (1991).
22. Stein, R., Boucsein, B. & Meyer, H. Anoxia and high primary productivity in the Paleogene central Arctic Ocean: first detailed record from the Lomonosov Ridge. *Geophys. Res. Lett.* **33,** L18606, doi:10.1029/2006GL026776 (2006).
23. Pearson, P. N. & Palmer, M. R. Atmospheric carbon dioxide concentrations over the past 60 million years. *Nature* **406,** 695–699 (2000).
24. Lowenstein, T. K. & Demicco, R. V. Elevated Eocene atmospheric CO_2 and its subsequent decline. *Science* **313,** 1928 (2006).
25. Abbot, D. S., Huber, M., Bousquet, G. & Walker, C. C. High-CO_2 cloud radiative forcing feedback over both land and ocean in a global climate model. *Geophys. Res. Lett.* **36,** L05702, doi:10.1029/2008GL036703 (2009).
26. Dunhill, G. Comparison of sea-ice and glacial-ice rafted debris: grain size, surface features, and grain shape. *US Geol. Surv. Open File Rep.* **OF 98-0367,** 1–82 (1998).
27. Williams, A. T. & Morgan, P. Scanning electron microscope evidence for offshore-onshore sand transport at Fire Island, New York, USA. *Sedimentology* **40,** 63–77 (1993).
28. Tripati, A. *et al.* Evidence for glaciation in the Northern Hemisphere back to 44 Ma from ice-rafted debris in the Greenland Sea. *Earth Planet. Sci. Lett.* **265,** 112–122 (2008).
29. Waddell, L. M. & Moore, T. C. Jr. Salinity of the Eocene Arctic Ocean from isotope analysis of fish bone carbonate. *Paleoceanography* **23,** PA1S12, doi:10.1929/2007PA001451 (2008).
30. Gleason, J. D. *et al.* Early to middle Eocene history of the Arctic Ocean from Nd-Sr isotopes in fossil fish debris, Lomonosov Ridge. *Paleoceanography* **24,** PA2215, doi:10.1029/2008PA001685 (2009).

Supplementary Information is linked to the online version of the paper at www.nature.com/nature.

Acknowledgements This research used samples and data provided by the Integrated Ocean Drilling Program (IODP). C.E.S. and N.K. acknowledge funding by VISTA (Norwegian Academy of Science and Letters and StatoilHydro) and the Research Council of Norway. We thank R. M. DeConto, M. P. Olney, S. M. Bohaty, A. Davies, M. A. Pearce, F. Sangiorgi, H. Brinkhuis, P. K. Bijl, J. Backman, J. Pike and A. E. S. Kemp for discussions. C.E.S. thanks StatoilHydro, Bergen for access to facilities, J. A. Barron, E. Fourtanier, I. Suto and J. Onodera for preliminary talks, and W. Hale for facilitating sample collection.

Author Contributions C.E.S. wrote the manuscript except for the sections on IRD and surface textures, which were written by K.S.J. and S.P. The manuscript incorporates comments by all authors, who also advised on its contents, structure and remit. Diatom analysis and light microscope imaging was undertaken by C.E.S.; statistical work on the surface textures was carried out by S.P.; R.B.P. and C.E.S. imaged *Synedropsis* spp. in the SEM at the NOCS; L.E.K. and K.S.J. undertook SEM analysis of surface textures; and SEM observations on *Synedropsis* spp. were also performed by R.W.J. and N.K.

Author Information Reprints and permissions information is available at www.nature.com/reprints. Correspondence and requests for materials should be addressed to C.E.S. (catherine.stickley@npolar.no).

METHODS

Quantitative IRD abundance. Bulk sediment samples were freeze-dried and weighed. Samples were wet-sieved and dried at 60 °C in an oven after which the sediment fractions were weighed. Visual estimates of the vol.% of the terrigenous abundance in the 150–250 and >250 μm fractions were made using a binocular microscope. The terrigenous grains in these sand-size fractions are considered to be IRD. The wt% IRD is calculated by multiplying the wt% abundance of the sand fraction (150–250 μm, or >250 μm) by the visual estimate of the abundance of terrigenous grains in the sand fraction.

Quantitative IRD surface texture analysis. A checklist approach[27,31] was used, involving photographing and recording the presence/absence of a series of features on every grain. Checklist categories are a hybrid from refs 26 and 27. The number of variables (textures) was reduced to result in a data set with as many sea-ice textures as iceberg textures and the values for all variables were normalized to between 0 and 1. Based on three principal components, accounting for ~50% of the variance in the data set, individual grains were classified as either sea-ice or iceberg sourced, based on the classification of ref. 26. For the discriminant analysis, grains were assigned to groups according to the PCA results.

31. Helland, P. E. & Diffendal, R. F. Jr. Probable glacial climatic conditions in source areas during deposition of parts of the Ash Hollow Formation, Ogallala Group (Late Tertiary), of Western Nebraska. *Am. J. Sci.* **293**, 744–757 (1993).